

# Practical Active Force Control with Iterative Learning Scheme Applied to A Pneumatic Artificial Muscle Actuated Robotic Arm

M. Mailah, H. M. Hooi, S. Kazi, H. Jahanabadi

**Abstract**— The precise motion control of a pneumatic artificial muscle (PAM) actuated system poses a great challenge to researchers due to the inherent nonlinearities, time-varying parameters, and high sensitivity to payload of the PAM mechanism. This paper highlights the effective practical implementation of an active force control (AFC) technique incorporating an iterative learning (IL) algorithm known as AFCAIL applied to a two-link planar robotic arm actuated by a pair of PAMs. The iterative learning is primarily used as a technique to compute the best value of the estimated inertia matrix of the robot arm required for the AFC loop that is complemented with a conventional proportional-integral-derivative (PID) control. An experimental rig utilizing a hardware-in-the-loop simulation (HILS) configuration was designed and developed based on suitable hardware and software installation. A number of experiments were carried out to validate the theoretical counterpart considering the independent joint control and coordinated motion control of the system for a given operating and loading conditions. The results of the experimental works verify the effectiveness and robustness of the proposed PAM actuated AFCAIL scheme in executing a number of trajectory tracking tasks.

**Keywords**— Active force control, hardware-in-the-loop simulation, iterative learning, pneumatic artificial muscle.

## I. INTRODUCTION

ROBOTS are typically designed to move objects through various programmed motions while performing specific tasks. Actuators are therefore indispensable components for all robotic systems since they provide the necessary forces, torques, and mechanical motions to move the joint, limb or body. Today's mechanical systems have such criteria for actuators including high power density, high power to weight ratio, rapid response, accurate and repeatable control, low cost, cleanliness and high efficiency. The pneumatic artificial muscle (PAM) actuator possesses many of these advantages, which is therefore considered as a strong candidate for robotic applications. However, the inherent nonlinearities, time-varying parameters, and high sensitivity to payload of the

PAM make it a challenge for the accurate force and position control of manipulators in employing these actuators. In order to have a proper control, the accurate model of actuator is needed. Hence, a number of researches have been carried out on the modelling of PAM for specific application. In [1], the principle of virtual work is used to derive the muscle force model and by [2] typical model as a parallel spring and a damper system is proposed and their mechanical behaviour was followed by [3]. With the aim of achieving satisfactory control performance, many control strategies have been proposed to deal with the effect of nonlinearity and hysteresis of PAMs. However, the majority of conventional control methods, such as PID controllers, are based on mathematical and statistical methods for modelling the system. In practice, the manipulators usually are highly nonlinear and a mathematical model may be difficult to obtain. Hence, conventional methods are not able to achieve high level of accuracy and robustness. Thanh and Anh in their research, proposed a nonlinear PID controller which was tuned by neural networks to control the two-link planar manipulator [4]. Recently, genetic algorithm is employed to identify the parameters of the two-link PAM manipulator by an ARX model [5]. Zhu *et al.* applied a discontinuous projection-based adaptive robust control method to control a three pneumatic-muscles-driven parallel manipulator through the simulation and experimental studies to achieve the precise posture trajectory tracking control [6]. An adaptive self-organizing fuzzy sliding mode control was developed by [7] that utilized a fuzzy sliding surface to reduce the number of fuzzy rules. Chan *et al.* has done an extensive simulation study on the control of PAM using fuzzy PD+I for position tracking of a vertical movement of a mass attached to a pneumatic muscle [8]. Lilly applied adaptive tracking techniques to PAM actuators arranged in bicep and tricep configurations [9]. As an extension to this work, a sliding mode control method for elbow angle tracking under load with PAM in place of the bicep and tricep configuration was employed [10]. Among the many research done on PAM, only a handful of research can be found pertaining to force control. Also, to the authors knowledge, there is as yet no available literature on the application of an iterative learning (IL) technique to control the PAM system directly or otherwise.

In this paper, a feedback control known as active force

Manuscript received 3 January, 2011; Revised version received 3 January, 2011. This work was supported by the Malaysian Ministry of Science, Technology and Innovation (MOSTI) and the Universiti Teknologi Malaysia under Project No. 03-01-06-SF0008.

All authors are with the Department of System Dynamics and Control, Faculty of Mechanical Engineering, Universiti Teknologi Malaysia, 81310 UTM Johor Bahru, Johor MALAYSIA (phone: +6075534735; fax: +6075566159; e-mail: [musa@fkm.utm.my](mailto:musa@fkm.utm.my)).

control (AFC) strategy is employed to control a PAM actuated robot system robustly and effectively. AFC has been recognized to be simple, robust and effective compared to conventional methods in controlling dynamical systems, both in theory as well as in practice through the pioneering works of Hewit and co-workers [11]. Their works were extended and consolidated by Mailah and fellow researchers, who applied the concept taking into account various value-added features to a number of dynamical systems which are mainly developed in the Systems and Control Laboratory at the *Universiti Teknologi Malaysia* (UTM) [12,13]. In this research, IL is incorporated into the control scheme to compute the estimated inertia matrix (IN) of a robot arm intelligently, so that it can be utilized by the AFC mechanism in compensating the disturbances. As an illustration, two types of motion control, namely, the independent joint control and coordinated motion control were considered and implemented. The AFCAIL schemes were subsequently benchmarked with the conventional PID counterparts with the main objective of acquiring robust and accurate trajectory tracking task performances.

II. PNEUMATIC ARTIFICIAL MUSCLE

The PAM in this research as an actuator is fluidic muscle produced by *FESTO* which is depicted in Fig. 1. The first idea of this type of actuator was proposed in the late 1950's by Gaylord for use in prosthetics and developed [14]. It was used by *McKibben* as an orthotic device for polio patients [15]. PAM is made up of a flexible rubber tube braided with cross-weave sheath material and two connection flanges. When the rubber tube is inflated with compressed air, the cross-weave sheath experiences lateral expansion, consequential in axial contractive force and the change of the end point position of PAM. Thus, the position or force control of the PAM along its axial direction can be found by regulating the inner pressure [6]. Its operation is very similar to how an animal skeletal muscle performs and is readily applicable to the construction of biomechanically realistic skeletal models [16].



Fig. 1 Fluidic muscle produced by FESTO

PAM actuators have been widely investigated with regard to static modelling and geometric calculations. Tondu and Lopez modelled the PAM actuator using the virtual work principle [1, 17] as depicted in Fig. 2. Ping and Hannaford also modelled the *McKibben* system using the principle of virtual work [18, 19] which is similar to Tondu and Lopez but they did not

separate the lateral force and axial force produced by internal pressure as shown in Fig. 2.

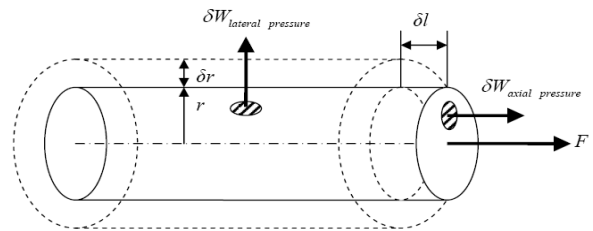


Fig. 2 Virtual work principle applied to *McKibben* actuator

The force produced by PAM can be expressed as a function of the total pressure  $P$  and contraction ratio  $\epsilon$  [1]:

$$F(P\epsilon) = (\pi r_0^2) P [a(1 - k\epsilon)^2 - b] \quad , \quad 0 \leq \epsilon \leq \epsilon_{max} \quad (1)$$

where  $P$  is the pressure inside the PAM,  $a$  and  $b$  are constants given by  $a = 3/\tan^2(\alpha_0)$  and  $b = 1/\sin^2(\alpha_0)$  respectively, that are related to the structure of PAM,  $k$  is a parameter to account for shape degradation at both ends of actuator during contraction,  $\epsilon$  is the contraction ratio expressed as  $\epsilon = (l_0 - l)/l$ ,  $r_0$  is the initial radius of the PAM, and the initial angle  $\alpha_0$  is defined as the angle between the PAM axis and each thread of the braided sheath before expansion .

III. DYNAMICS OF THE ROBOTIC ARM

The dynamics of the manipulator is not completely consistent with that of a human arm. By modelling the coupled links as a conservative system, friction is neglected which is inherent in realistic applications. In addition, the computational model is unable to impose the geometric constraints characteristic of the human joints. The applicability of *Lagrange's* equation of motion in robotics is demonstrated by modelling the two-link planar robotic arm as shown in Fig. 3.

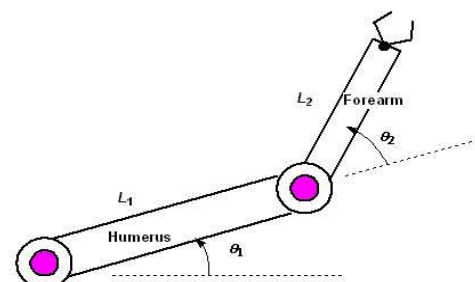


Fig. 3 A representation of a two link robotic arm

In the figure, subscripts 1 and 2 refer to the parameters of the first link (Humerus) and second link (forearm), respectively.  $L$  is the length of arm and  $\theta$  is the angular (joint) position of the arm. *Lagrange* formulation is used to derive the equation of motion for the nonlinear dynamic system. The general dynamic equation for a series rotating manipulator can

be described as follows [20]:

$$\tau = \mathbf{H}(\theta)\ddot{\theta} + \mathbf{h}(\theta, \dot{\theta}) + \mathbf{G}(\theta) + \tau_d \quad (2)$$

Where  $\tau$  is the actuated torque vector,  $\mathbf{H}$  is the  $N \times N$  inertia matrix of the manipulator,  $\mathbf{h}$  is the *Coriolis* and centripetal torque vector,  $\mathbf{G}$  is the gravitational torque vector and  $\tau_d$  is the external disturbance torque vector. Since the arm is assumed to move in a horizontal plane, the gravitational term can be omitted.

The detailed dynamic model is given by:

$$\tau_1 = H_{11}\ddot{\theta}_1 + H_{12}\ddot{\theta}_2 - h\dot{\theta}_2^2 - 2h\dot{\theta}_1\dot{\theta}_2 \quad (3)$$

$$\tau_2 = H_{22}\ddot{\theta}_2 + H_{21}\ddot{\theta}_1 - h\dot{\theta}_1^2 \quad (4)$$

Where

$$H_{11} = m_2 l_{c1}^2 + I_1 + m_2(l_{c1}^2 + l_{c2}^2 + 2l_1 l_{c2} \cos\theta_2) + I_2 \quad (5)$$

$$H_{12} = H_{21} = m_2 l_1 l_{c2} \cos\theta_2 + m_2 l_{c2}^2 + I_2 \quad (6)$$

$$H_{22} = m_2 l_{c2}^2 + I_2 \quad (7)$$

$$h = m_2 l_1 l_{c2} \sin\theta_2 \quad (8)$$

#### IV. ROBOTIC ARM ACTUATED BY ANTAGONISTIC PAMS

Two PAMs arranged into an antagonism configuration emulate a physiological model of the bicep-tricep system – the antagonistic configuration of skeleto-muscle system of human elbow joint. The two muscles are connected by a timing belt driven a timing pulley. The differential pressure and in consequence, force difference between the agonist and the antagonist produces a positive or negative torque. Both muscles shall pressurize at the same pressure  $P_0$  and cause the same contraction ratio  $\varepsilon_0$  in the first place. When the agonist inflates with pressure  $P_1$  different from the antagonist pressure  $P_2$ , an actuator rotation of angle  $\theta$  shall be produced. This principle is depicted in Fig. 4.

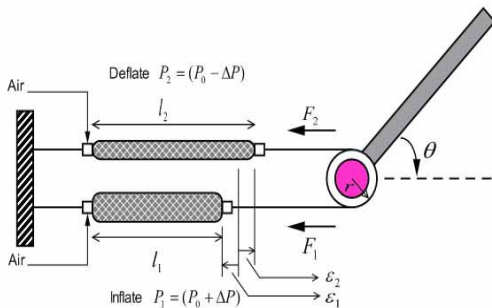


Fig. 4 Working principle of antagonistic fluidic muscle actuator

A model of produced torque by the actuators can be managed by force produced by each actuator. The agonist force will be denoted  $F_1$ , the antagonist force  $F_2$ , and the

timing pulley radius  $r$ . We obtain:

$$\tau = (F_1(\varepsilon_1, P_1) - F_2(\varepsilon_2, P_2))r \quad (9)$$

$$\varepsilon_1 = \varepsilon_0 + r\theta/l_0, \varepsilon_2 = \varepsilon_0 - r\theta/l_0 \quad (10)$$

After developing the torque model in above, a monovariable approach of the PAM actuator, which could be called symmetrical co-contraction by analogy with the neurophysiological terminology is now considered. The symmetrical pressure variation, applied from initial pressure  $P_0$  in both muscles, will be noted  $\Delta P$ . By applying  $P_1 = P_0 + \Delta P$  and  $P_2 = P_0 - \Delta P$  in (10), the torque model of the actuator becomes:

$$T = 2K_1 \Delta P - 2K_2 P_0 \theta \quad (11)$$

Where

$$K_1 = (\pi r_0^2) r [a(1 - k\varepsilon_0)^2 - b] \quad (12)$$

$$K_2 = (\pi r_0^2) r 2a(1 - k\varepsilon_0)kr/l_0 \quad (12a)$$

This model highlights the main originality of the actuator. The static relationship is deduced with  $G$  representing an open-loop gain [1]:

$$\theta = G \Delta P \quad (13)$$

$$G = \frac{K_1}{K_2} = \frac{l_0 [a(1 - k\varepsilon)^2 - b]}{2akr(1 - k\varepsilon_0)P_0} \quad (14)$$

The schematic model of a two link planar driven by PAMs can be seen in Fig. 5. In this model, each link is actuated by a pair of PAM that the differential pressure causes to move the link. For first link the actuator is fixed to the body while the second link's muscles are attached to the first link.

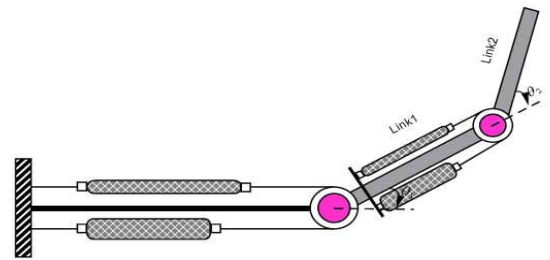


Fig. 5 Schematic model of the PAM actuated two link arm system

#### V. CONTROLLER DESIGN

In this section, all the major elements constituting the design and implementation of the overall control system are described. It involves three stages; firstly, the design of the PID controller; secondly, the integration of AFC into the PID control system and lastly, the incorporation of an iterative



The idea behind the AFCAIL scheme is to obtain a continuous computation of the estimated inertia matrix of the arm by means of a suitable learning algorithm in which the arm is gradually forced to execute a prescribed task accurately even in the presence of unknown disturbances. As the arm starts to move, the internal mechanism activates the learning process by identifying new inertia values of the links for each iteration after which these signals were then processed by the AFC loop, thereby performing the required task and eventually reducing the track error. This error is in turn fed back into the learning algorithm section and the process is repeated iteratively until a suitable error goal criterion is achieved. The estimated inertia matrix  $IN$  is updated iteratively and the track error  $TE$  is forced to converge to value approaching zero as the learning progresses and the robot arm continuously moves to describe a predefined input reference.

A flow chart showing the logical flow of the main algorithm is illustrated in Fig. 9. Information about the robot's trajectory or motion while performing a specific task is relayed to a feedback in the outer control loop of the overall control scheme as the robot moves. This information is compared with the desired reference input and the difference between the two gives the track error. The resulting track error is then used by the IL algorithm to determine the inertia matrix of the arm for the next cycle.

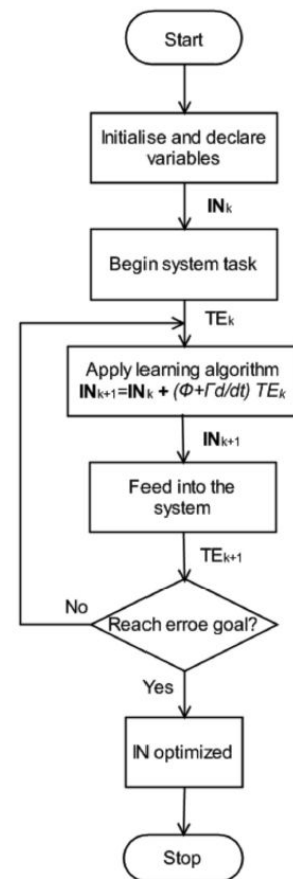


Fig. 9 A PD type learning algorithm applied to robot arm

## VI. SIMULATION

All the controller parameters (PID, AFC and IL) need to be obtained prior to the implementation of the overall scheme. It is assumed that the main controller parameters were adequately tuned after a number of standard procedures. Then, these parameters were incorporated into the scheme and later experimented via the hardware-in-the-loop simulation (HILS) configuration. The parameters used in the study are presented in the following sections.

### A. PID Parameters

Table 1 shows the PID parameters that were derived from works done in [24].

Table 1 PID parameters for the PAM system

PID Parameter	Value
Proportional gain of link 1, $K_{P1}$	21
Integral gain of link 1, $K_{I1}$	35
Derivative gain of link 1, $K_{D1}$	3.15
Proportional gain of link 2, $K_{P2}$	30
Integral gain of link 2, $K_{I2}$	42.86
Derivative gain of link 2, $K_{D2}$	5.25

**B. Link Parameters**

The main link parameters of the robotic arm can be seen in Table 2.

Table 2 Link parameters

$m_1$	Mass of link1	1.25 kg
$m_2$	Mass of link 2	0.75 kg
$L_1$	Length of link1	0.405 m
$L_2$	Length of link 2	0.290 m

**C. IL Parameters**

The IL learning parameters were set as follows:

$$\Phi = 0.0175, \Gamma = 0.005$$

Initial conditions:  $IN1 = 0.4 \text{ kgm}^2$  and  $IN2 = 0.04 \text{ kgm}^2$

It is useful to note that in the IL algorithm, one has to consider the initial conditions to commence the iterating process. The initial conditions refer to the instances where the system starts from 0 second. i.e., the robot arm is at rest position. It is essential that appropriate initial conditions are specified in order to obtain the desired behaviour of the system. For the IL algorithm, although  $IN$  can be assumed the same initial value, it is clear that from the robot's physical configuration,  $IN1$  is realistically greater than  $IN2$ . It is verified in [18] that  $IN1 > IN2$  produced more accurate results than  $IN1 = IN2$ . A stopping criterion is also specified for halting the learning process if the convergence of the desired parameter is assumed to have taken place. The range of the track error set for the system's performance deemed to be acceptably accurate and stable is  $0 \leq TE \leq 0.0174 \text{ rad}$  ( $0 \leq TE \leq 1 \text{ degree}$ ). The Simulink model of the AFCAIL scheme is shown in Fig. 10.

sensors, actuators and other electronic devices were processed through the analogue to- digital and digital-to-analogue converters functions which were already embedded in the card. A pair of pneumatic artificial muscle (MAS-10-N-250-AA-MCFK) and a pair of pneumatic artificial muscle (MAS-10-N-100-AA-MCFK) were used as actuators. To control the pressure, the proportional pressure regulators were used as the servovalves. The advantage of using the proportional pressure regulator is that no pressure sensor is required because of its built-in pressure controller. Therefore, mathematical formulation of the pneumatic flow is not required. In the rig set-up, proportional pressure regulators (MPPEs-3-1/8-10-010) were utilized to control the pressure inside the PAMs. Accelerometers (ADXL330) were used to measure the acceleration of each link. The physical sensors and actuators required for the input/output (I/O) signals were connected to a PC-based data acquisition and control system via MATLAB/Simulink/Real Time Workshop (RTW) and other related components that essentially constitute the hardware-in-the-loop simulation (HILS) configuration. Fig. 11 shows the RTW processing part of the PAM system.

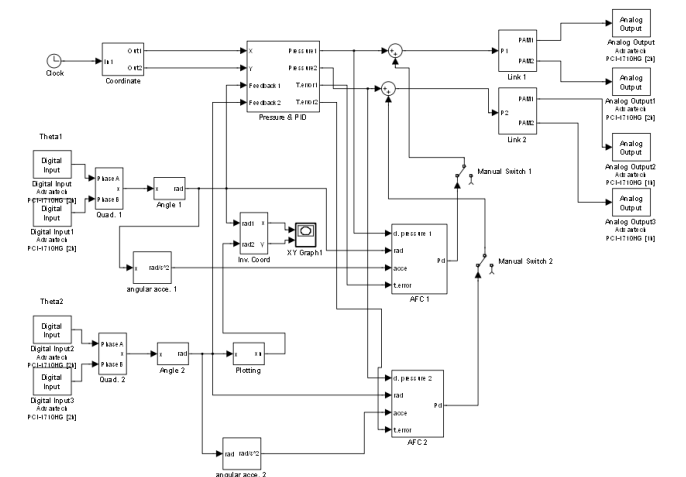


Fig. 11 Simulink model with RTW

Fig. 12 illustrates a view of the physical rig while Fig. 13 depicts a schematic representation of the experimental set-up.

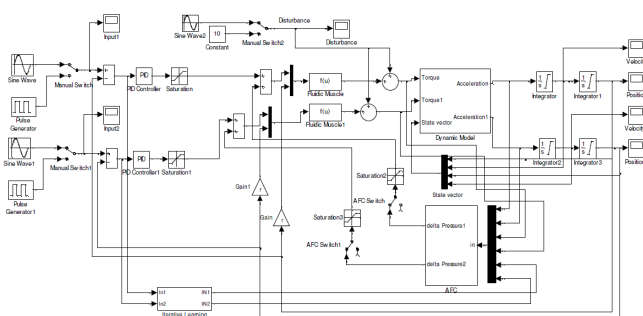


Fig. 10 Simulink model for the AFCAIL scheme

**VII. EXPERIMENTAL SETUP**

This section presents the practical feature of rig based on the proposed control strategy. Two data acquisition board (PCI-1710HG) were used. Appropriate signals from the

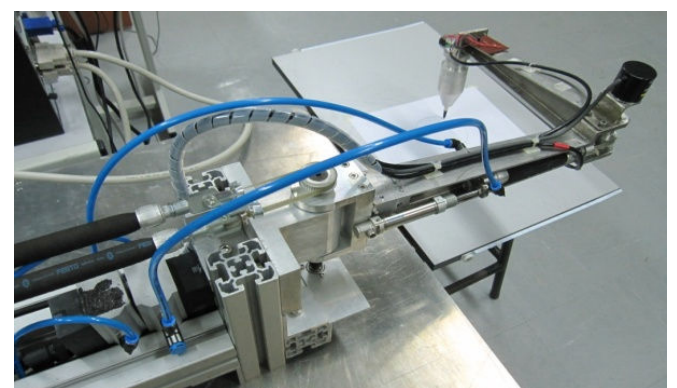


Fig. 12 A view of the physical rig

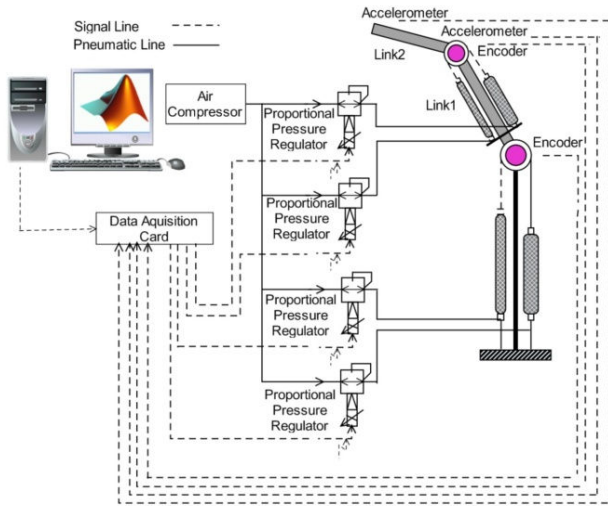


Fig. 13 Schematic diagram of the experimental set-up

Two types of experiments were carried out:

1. Independent joint control of the first link at frequency,  $f = 0.1$  Hz with a harmonic disturbance,  $Q = 10 \sin(2t)$  Nm (joint space). The experiment is repeated for  $f = 0.05$  and  $0.2$  Hz for the second link.
2. Coordinated motion control of the arm (in *Cartesian* or task space) performing a circular trajectory tracking task with a spring disturbance,  $k_s = 50$  N/m

Prior to applying the controller, all muscles were pressurized to 4 bar. Due to the same pressure in each PAM, the torque is initially set to zero. Two types of control algorithms, namely, the PID and AFC with IL were applied individually with the former executed first, followed by the latter.

### VIII. RESULTS AND DISCUSSION

The robustness and viability of AFC-based scheme were satisfactorily carried out through the experimental study using a number of appropriate parameters obtained through a number of standard techniques or operating procedures. Fig. 14 shows that the PID scheme for the independent joint control of link 1 produces significant track errors as it does not satisfactorily conform to the desired joint trajectory throughout the simulation period. On the other hand, Fig. 15 illustrates the superiority of the AFCAIL scheme to track the sinusoidal trajectory. The actual trajectory generated almost replicates the desired counterpart. Similar trend is also observed in both Figs. 16 and 17 for different frequencies related to the second link trajectories for the given experimental conditions. It is very evident that the AFCAIL produces a rapid response, indicating that all the mechanisms (including the IL part) work to ‘perfection’.

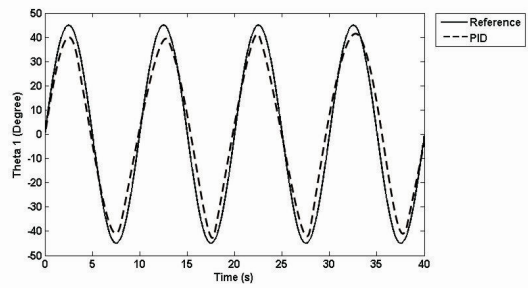


Fig. 14 PID performance for link 1 at  $f = 0.1$  Hz

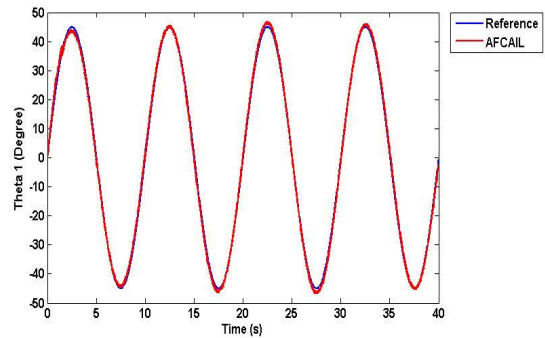


Fig. 15 AFCAIL performance for link 1 at  $f = 0.1$  Hz

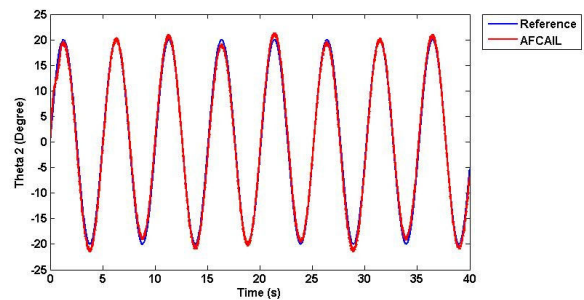


Fig. 16 AFCAIL performance for link 2 at  $f = 0.2$  Hz

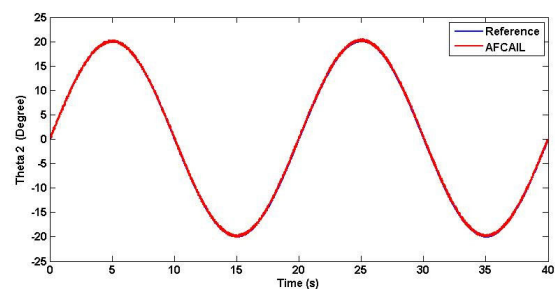


Fig. 17 AFCAIL performance for link 2 at  $f = 0.05$  Hz

For the coordinated motion control, the arm was designed to perform a circular trajectory with a radius of 5 cm and a driving frequency of 0.1 Hz as depicted in Fig. 18. This low frequency setting ensures that the proposed system has a low speed tracking motion to compensate for the hysteresis behaviours of the actuators. The mean track errors obtained for this experiment are 0.0013 m and 0.0009 m for PID and AFCAIL schemes, respectively, as shown in Fig. 19. Again, the AFC-based control system performs better than the PID

counterpart. Fig. 20 shows the computed estimated inertia of link 1 which illustrates a crude sinusoidal pattern as it describes the circular path.

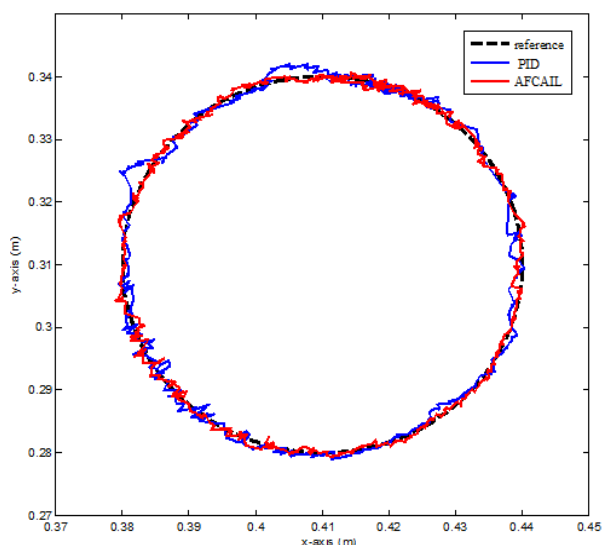


Fig. 18 Circular tracking results with spring disturbance: (a) reference, (b) PID and (c) AFCAIL

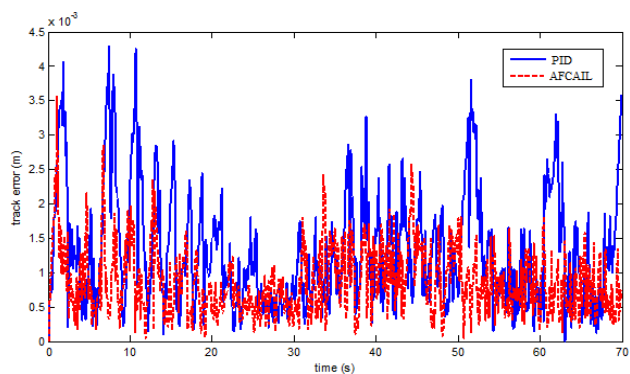


Fig. 19 Tracking errors for the circular trajectory

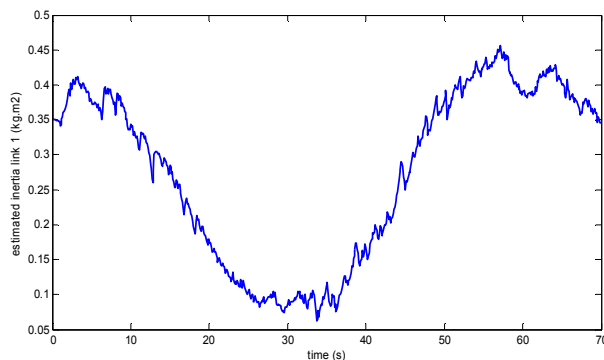


Fig. 20 Computed estimated inertia of link 1 via AFCAIL

The proposed scheme clearly demonstrates their robustness and effectiveness to control the robot arm equipped with the highly non-linear PAM actuators. The IL part is also very effective in estimating the IN continuously on-line as the robot operates. This clearly shows that the AFC-based

systems produce excellent results for effective tracking control even in the wake of inherent hysteresis behaviour, non-linearities and disturbances in the PAM system.

## IX. CONCLUSION

The proposed practical AFCAIL controller based on a HILS concept has been shown to perform effectively when implemented to the real-time control of a two axes planar robotic arm driven by PAMs. The experimental results verify the robustness of the AFC-based algorithms in performing the independent joint and coordinated motion trajectory tracking control tasks. The proposed schemes perform much better than the standard PID control technique. One of the main research contributions was the effective control of the PAM actuated system through the AFC-based schemes considering the presence of the inherent non-linearities and disturbances in the system. Future works shall take into account other forms of disturbances, different operating conditions and parametric changes.

## REFERENCES

- [1] B. Tondu and P. Lopez, "Modeling and control of McKibben artificial muscle robot actuators," *IEEE Control Systems Magazine*, vol. 20, pp. 15-38, 2000.
- [2] D. B. Reynolds, D. W. Repperger, C. A. Phillips, and G. Bandry, "Modeling the dynamic characteristics of pneumatic muscle," *Annals of Biomedical Engineering*, vol. 31, pp. 310-317, 2003.
- [3] K. C. Wickramatunge and T. Leephakpreeda, "Study on mechanical behaviors of pneumatic artificial muscle," *International Journal of Engineering Science*, vol. 48, pp. 188-198, 2010.
- [4] T. U. D. C. Thanh, and K. K. Ahn, "Nonlinear PID control to improve the control performance of 2 axes pneumatic artificial muscle manipulator using neural network," *Mechatronics*, vol. 16, pp. 577-587, 2006.
- [5] K. A. Kyoung and P. H. A. Ho, "System identification and self-tuning pole placement control of the two-axes pneumatic artificial muscle manipulator optimized by genetic algorithm," in *Procs. of Int'l Conference on Mechatronics and Automation*, 2007pp. 2604-2609.
- [6] X. Zhu, G. Tao, B. Yao, and J. Cao, "Adaptive robust posture control of a parallel manipulator driven by pneumatic muscles," *Automatica*, vol. 44, pp. 2248-2257, 2008.
- [7] M. K. Chang, "An adaptive self-organizing fuzzy sliding mode controller for a 2-DOF rehabilitation robot actuated by pneumatic muscle actuators," *Control Engineering Practice*, vol. 18, pp. 13-22, 2010.
- [8] S. W. Chan, J. H. Lilly, D.W. Repperger, and J. E. Berlin, "Fuzzy PD+I learning control for a pneumatic muscle," in *Procs. of the 12th IEEE Int'l Conference on Fuzzy Systems*, vol.1, 2003, pp. 278-283.
- [9] J. H. Lilly, "Adaptive tracking for pneumatic muscle actuators in bicep and tricep configurations," *IEEE Trans. on Neural Systems and Rehabilitation Engineering*, vol. 11, pp. 333-339, 2003.
- [10] J.H. Lilly and Y. Liang, "Sliding mode tracking for pneumatic muscle actuators in opposing pair configuration," *IEEE Trans. on Control Systems Technology*, vol. 13, pp. 550-558, 2005.
- [11] J. R. Hewit and J. S. Burdess, "Fast dynamic decoupled control for robotics using active force control," *Mechanism and Machine Theory*, vol. 16, pp. 535-542, 1981.
- [12] E. Pitowarno, M. Mailah, and H. Jamaluddin, "Knowledge-Based Trajectory Error Pattern Method Applied to An Active Force Control Scheme," *International Journal of Engineering and Technology*, vol. 2, pp. 1-15, 2002.
- [13] M. Mailah, H. J. Abadi, M. Z. M. Zain, and G. Priyandoko, "Modelling and control of a human-like arm incorporating muscle models", *Proceedings of the Institution of Mechanical Engineers, Part C: Journal of Mechanical Engineering Science*, vol. 223, pp. 1569-1577, 2009.

- [14] R. H. Gaylord, 1958. Patent, No 2,944,126. United States patent application.
- [15] V. L., Nickel, J. Perry, and A. L. Garret, "Development of useful function in the severely paralyzed hand," *The Journal of Bone and Joint Surgery*, vol. 45A, pp. 933-952, 1963.
- [16] D. W. Repperger, C. A. Phillips, A. Neidhard-Doll, D. B. Reynolds, and J. Berlin, "Actuator design using biomimicry methods and a pneumatic muscle system," *Control Engineering Practice*, vol. 14, pp. 999-1009, 2006.
- [17] B. Tondu and P. Lopez, "Modeling and control of McKibben artificial muscle robot actuators," *IEEE Control Systems Magazines*, vol. 20, pp. 15-38, 2000.
- [18] C. C. Ping and B. Hannaford, "Measurement and modeling of McKibben pneumatic artificial muscles," *IEEE Trans. on Robotics and Automation*, vol. 12, pp. 90-102, 1996.
- [19] C. C. Ping and B. Hannaford, "Static and dynamic characteristics of McKibben pneumatic artificial muscles," in *Procs. IEEE International Conference on Robotics and Automation*, 1994, vol.1, pp. 281-286.
- [20] J. J. Craig, *Introduction to Robotics: Mechanics and Control*. Pearson Prentice Hall, 2005.
- [21] S. Arimoto, "Learning control theory for robotic motion," *International Journal of Adaptive Control and Signal Processing*, vol. 4, pp. 543-564, 1990.
- [22] S. Arimoto, S. Kawamura, and F. Miyazaki, "Convergence, stability and robustness of learning control schemes for robot manipulators," in *Procs. of the Int'l Symposium on Robot Manipulators and Recent Trends in Robotics: Modeling, Control and Education*. Albuquerque, New Mexico, USA, 1986.
- [23] M. Mailah, "Intelligent active force control of a rigid robot arm using neural network and iterative learning algorithms," PhD Thesis, Dept. of APEME, University of Dundee, UK, 1998.
- [24] H. Jahanabadi, M. Mailah, M. Z. M. Zain, and H. H. Mun, "Active force with fuzzy logic control of a two-link arm driven by pneumatic artificial muscles," *Journal of Bionics Engineering*, vol. 8, 2011.